Optimization design and experiment of double-helix total mixed rations preparation mixer for silage straw feed

Meizhou Chen,[1] Guangfei Xu,[2] Xianghao Li,[1] Hongda Zhao,[1] Yongli Zhao,[1] Peisong Diao,[1] Yinping Zhang[1]

[1]College of Agricultural Engineering and Food Science, Shandong University of Technology, Zibo, China; [2]School of Mechanical and Automotive Engineering, Liaocheng University, China

Abstract

The traditional vertical single-helix mixer for silage straw feed was replaced with a double-helix total mixed ration (TMR) preparation mixer, which aims to address the issues of uneven mixing and low production efficiency of domestic silage mixers. This preparation machine was used for the performance tests and parameter optimization. The main elements influencing the range and mixing performance were identified by dissecting the diets' mechanism and mixing process inside the mixing chamber. The more the churn's stirring speed and material lift angle, the more favorable it was discovered that the churn device was for increasing its capacity to lift materials. Using EDEM simulation software, the preparation machine's mixing properties and material movement were numerically simulated, and the preparation machine's mixing effect was confirmed. The prototype's three-factor and five-level central composite design center combination orthogonal rotary test was conducted using the following evaluation metrics: ton material energy consumption, roughage particle size, mixing uniformity, and filling coefficient as evaluation indices; stirring speed of the churn, mixing time, and filling coefficient as influencing factors. The test results demonstrated that the filling coefficient, stirring speed, and mixing time contributed descending order to mixing uniformity; the stirring speed, mixing time, and filling coefficient contributed descending order to roughage particle size; and the filling coefficient, mixing time, and stirring speed contributed descending order to the ton material energy consumption. The optimal working parameters for mixing performance by comprehensive optimization could be concluded as stirring speed of 48.59 r/min, mixing time of 14.98 min, and filling coefficient of 70%. In addition, the mixing uniformity, roughage particle size, and ton material energy consumption were obtained as 91.11%, 72.13%, and 2.99 kW·h/t. The relative error for all evaluation indexes between the experimental results with round parameter combination and the predicted value was verified to be less than 3%. As can be observed, the double-helix TMR preparation mixer can effectively meet the demand for silage straw feed mixing. This, in turn, offers technical support and data references for the design and selection of TMR preparation machine operating parameters.

Correspondence: Peisong Diao, College of Agricultural Engineering and Food Science, Shandong University of Technology., 266 Xincun Road, Zibo, China.
E-mail: dps2003@163.com

Key words: TMR; preparation mixer; double-helix; mechanistic analysis; parameter optimization.

Acknowledgments: the authors would like to thank LetPub (www.letpub.com) for its linguistic assistance during the preparation of this manuscript.

Contributions: all the authors contributed equally.

Conflict of interest: the authors declare no potential conflict of interest.

Funding: this study was supported by the Shandong Provincial Natural Science Foundation (ZR2023QE091).

Availability of data and material: data and material are available from the corresponding author upon request.

Received: 3 August 2023.
Accepted: 9 February 2024.

Journal of Agricultural Engineering 2024; LV:1567
doi:10.4081/jae.2024.1567

Introduction

China is one of the countries with a high stock of dairy cows in the world. Traditional dairy farming generally adopts the feeding method of concentrate and roughage, which is easy to cause metabolic diseases and affect the quality of milk products (Wang *et al.*, 2020; Schingoethe *et al.*, 2017). Total mixed ration (TMR) is a kind of feeding technology according to the nutritional requirements of ruminant livestock at different physiological stages, mixing concentrate, roughage, and various feed additives according to a certain ratio, and then sent to the loose stalls by the feeding truck for livestock to feed freely, which saves labor and time, and can increase the yield by 7~10% (Tian *et al.*, 2020a; Wang *et al.*, 2019).

At present, TMR feeding technology is commonly used in countries with developed animal husbandry in the world, such as the United States, Canada, Israel, Germany, Norway, France, the Netherlands, Italy, and other countries. This technology was introduced into China relatively late, and domestic enterprises have developed vertical and horizontal total mixed diet preparation machines by following the mature technology of foreign countries. In recent years, domestic research institutes, colleges and universities and enterprises have made some achievements in TMR technology and equipment. In terms of improving mixing efficiency, the churns are dominated by single-shaft horizontal type (Frizzarin *et al.*, 2021), single-shaft vertical type (Jiang *et al.*, 2022), leaf-plate type (Chen *et al.*, 2022), rotating type (Wang *et al.*, 2020), etc. In terms of traveling system, traction (Wang *et al.*, 2017a; Li *et al.*, 2017) and self-propelled (Wang et al., 2017b; Tian *et al.*, 2020a) are the main research objects (*Supplementary Table 1*). Some related companies based on existing foreign models, mainly for small-scale pasture production of single-screw vertical and three-screw horizontal TMR preparation machine, a single type (Niu *et al.*, 2022). Domestic research on self-propelled TMR preparation machine lacks research on the mixing mechanism and optimization method, not to overcome the key technology and not to form industrialization. In order to solve the above challenges, this article focuses on exploring the structural advantages of the vertical double agitator structure for feed mixing.

In this case, a double-helix TMR preparation mixer for silage straw feed was developed to solve technical problems of the TMR preparation machine at the present stage in China. The structural parameters and operating parameters affecting its material mixing performance are determined through dynamics, kinematics, and EDEM simulation. The optimal working parameter combinations of the preparation machine were obtained through the multi-factor test of the prototype, and the reliability of the mixing performance was verified, to provide a reliable data reference and theoretical basis for the development of the TMR preparation machine.

Materials and Methods

Main structure

The scheme of the double-helix TMR preparation mixer for silage straw feed is shown in Figure 1, including the mixing tank, stirring device, dumping device, transmission system, weighing system trailed chassis, and other components. The trailed chassis has a front-mounted towing unit hooked up to the tractor with running wheels at the rear. The mixing tank is located at the rear end of the tractor, and the bottom of the mixing tank is connected to the trailed chassis by means of a gravity sensor. The mixing tank has a ladder welded to one side of the outer wall, a removable fixed knife at each of the front and rear curved end plates, and two symmetrically distributed vertical conical helix churn inside. The bottom end of the stirring device is bolted to the variable gearbox, and the tractor transmits the power to the stirring device through the transmission lever and the variable gearbox, and the stirring device rotates in the direction from the bottom up. The weighing system consists of a weight indicator and 4 load cells distributed evenly on the bottom plate of the mixing tank. The dumping device is mounted at the curved end plate in front of the mixing box and is powered by a hydraulic motor.

Work principle

The test physical prototype is shown in Figure 2. Through full investigation and selection design calculation in the early stage, the main technical parameters of the double-helix TMR preparation mixer are determined as shown in *Supplementary Table 2*.

During operation, the tractor transmits the power to the stirring device through the transmission lever and the variable gearbox, which drives the churns to rotate in the opposite direction. Then the material to be mixed is put into the mixing tank by the loading machine, and the amount of material is controlled by the weighing system. With the rotation of the churn, the movable blade on the spiral blade and the adjustable fixed knife on the wall of the material box form a shearing surface. The relative movement of the adjustable fixed knife forms a shear surface, which can cut the long fiber material. In the process of rising, under the action of centrifugal force, the material will be thrown radially along the churn spiral blade, falling to the bottom of the mixing tank. The material is cut and mixed by the churn spiral blade repeatedly. Strong convec-

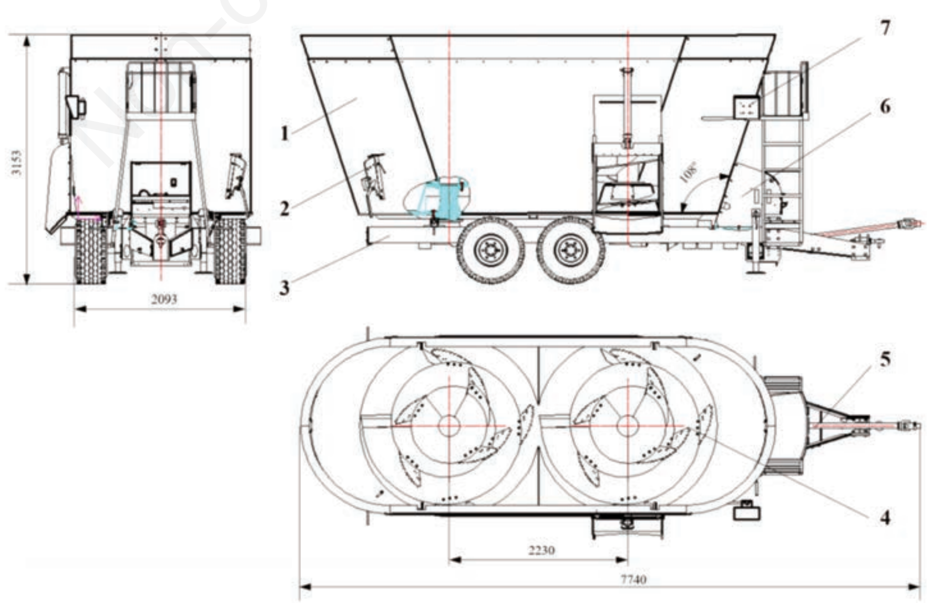

Figure 1. Structure diagram of double-helix total mixed ration preparation mixer. 1) Mixing tank; 2) fixed blade; 3) trailed chassis; 4) stirring device; 5) transmission system; 6) dumping device; 7) weighing system.

tion mixing, diffusion mixing and shear mixing will be generated to achieve rapid and uniform mixing. After mixing, start the hydraulic system, and open the unloading door at the same time, the hydraulic motor drives the feeding device begins to work, the mixture will be thrown to the designated location, and then the feeding process is completed.

Structural design of double-helix churns

The main function of the stirring device is to lift the material from the bottom of the mixing tank to the top. The churn is the core component of the stirring device. The structure adopts isometric spiral conical design and horizontal arrangement, which mainly consists of spiral sleeve, spiral blade, movable blade, and knife pallet (Figure 3).

Four spiral blades are welded to the spiral sleeve. The first spiral blade is installed with 1 movable blade, which plays the role of scraping and lifting. The second and third spiral blades are installed with 5 movable blades evenly distributed on the blades, which play the role of cutting and lifting. The fourth spiral blade is installed with 2 movable blades, which play the role of sweeping and cutting. In order to prevent the blade from loosening, reduce wear and increase its service life, a blade carrier is installed underneath each movable blade.

Double-helix churns design analysis

Mixing mechanism analysis

The mixing process is shown in Figure 4. During the mixing process, the material was divided into three parts from bottom to top: driving layer, permeable layer and stranded layer. The churn blade was a vertical conical spiral structure with a decreasing loading surface from bottom to top. A portion of the driving layer material in the process of rising along the radial diffusion around the cone, with the permeable layer material mixing. The other part of the driving layer of material along the churn blade movement to the top of the stirring device and then diffuse, and stranded layer material for mixing. As the material at the bottom of the mixing tank was gradually lifted by the spiral blade, the material of the stranded and the permeable layer completed the filling under the action of their own gravity in a continuous cycle.

Kinematic analysis

Assuming that there was any point in the mixing tank of material particles M, under the action of the spiral blade to do the compound motion, the motion analysis is shown in Figure 5. A dynamic reference system $x'y'z'$ is established with the spiral blade and a static reference system xyz is established with the mixing tank.

The lifting capacity of the stirring device is expressed by the axial speed of the material. The larger the axial speed of the material, the stronger the lifting capacity. Therefore, the axial velocity $v_{z'}$ of M was analyzed. In the normal conveying process, the relationship between the absolute velocity v_a, the implicated velocity v_e and the relative velocity v_r of the particles M was as follows:

$$\begin{cases} \dfrac{v_a}{\sin\alpha} = \dfrac{v_e}{\sin(\alpha+\beta)} = \dfrac{v_r}{\sin\beta} \\ v_e = \omega r = \pi n r / 30 \end{cases} \tag{1}$$

where, n is the stirring speed (r/min); β is the material movement angle of lifting (°); ω is the churn blade angular velocity (rad/s); α is the churn blade helix angle of rising (°); r is the radius of rotation of the location of M (m).

The circumferential velocity $v_{x'}$ and axial velocity $v_{z'}$ of M are as follows respectively:

$$v_{z'} = v_a \sin\beta \tag{2}$$

$$v_{x'} = v_a \cos\beta \tag{3}$$

It is obtained by Eq. 1-3:

$$v_{z'} = \frac{\pi n r}{30(\cot\alpha + \cot\beta)} \tag{4}$$

According to Eq. 4, the axial velocity $v_{z'}$ of M was related to the stirring speed n, the radius of rotation r of the position where M is located, the churn blade helix angle of rising α of the spiral blade and the material movement angle of lifting β. In the case that the structural parameters of the stirring device were determined, the axial velocity $v_{z'}$ increased with the increase of the stirring speed n and the material movement angle of lifting β. However, the relationship between n and β was not yet known, and it was necessary to analyze further to get the relationship between the two changes.

Figure 2. Physical prototype.

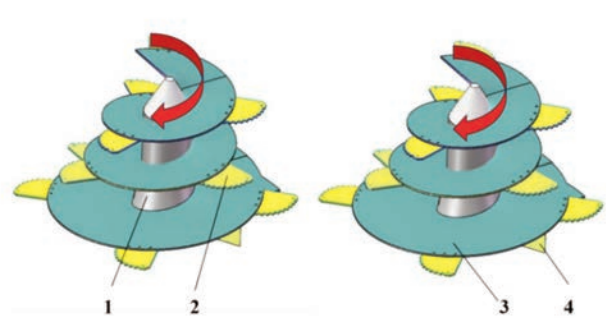

Figure 3. Schematic diagram of double-helix churns structure. 1) Churn shaft; 2) movable blade; 3) spiral blade; 4) scraper.

Kinetic analysis

The force analysis of the particle M in general position is carried out as shown in Figure 6.

Mechanical equilibrium Equations were established on the x', y', and z' axes of the dynamic reference system, respectively as follows:

$$F_2\cos\beta - F_1\cos\alpha - F_{N_1}\sin\alpha = 0 \tag{5}$$

$$F_{N_1} - F_e = 0 \tag{6}$$

$$F_{N_1}\cos\alpha - mg - F_1\sin\alpha - F_2\sin\beta = 0 \tag{7}$$

where,

$F_2 = \tan\delta F_{N2}$, $F_1 = \tan\gamma F_{N1}$, $F_e = mv_{x'}^2 / r$, $v_{x'} = v_a\cos\beta = v_e\sin\alpha\cos\beta / \sin(\alpha+\beta)$

where, γ is the friction angle between churn blade and material(°); δ is the angle of internal friction of the material(°).

It is obtained by Eqs. 5-7:

$$900g\sin(\alpha+\gamma)\left(1+\frac{\tan\beta}{\tan\alpha}\right)^2 = n^2\pi^2\gamma\tan\delta\cos(\alpha+\beta+\gamma) \tag{8}$$

From Eq. 8, it can be seen the material movement angle of lifting β was related to the stirring speed n, the churn blade helix angle of rising α, the radius of rotation of the location r, the angle of internal friction of the material δ, and the friction angle between churn blade and material γ. To obtain the relationship between both β and n, α was set to be 5°, r to be 1 m, δ to be 75°, and γ to be 20°. The curve of β as a function of n is fitted and the results are shown in Figure 6.

As can be seen from Figure 7, with the increase of the stirring speed, the material movement angle gradually increased, and the material lifting capacity of the stirring device was enhanced. The stirring speed should not be too large, otherwise the energy consumption would increase, the equipment would accelerate the wear and tear, and the service life would be shortened.

From the above analysis, it can be seen when β>0, the material at the bottom of the mixing tank can be pushed to the top by the blades. When β=0, the material was neither up nor down, at this time the material relative to the blade was stationary, seriously affecting the mixing effect of material. Therefore, when β=0, there existed a minimum value of the churn speed, *i.e.*, the critical speed n_0.

From Eq. 8, n_0 can be expressed as follows:

$$n_0 = \frac{30}{\pi}\sqrt{\frac{g\tan(\alpha+\gamma)}{r\tan\delta}} \tag{9}$$

From Eq. 9, the critical speed n_0 was related to α, r, δ, and γ. The critical speed n_0 increased as the churn blade helix angle of rising α increased and increased as the radius of rotation of the location r decreased. The spiral blades have a conical spiral structure with a decreasing radius of rotation from the bottom up. In order to make the churn blade meet the same critical speed as far as possible, the helix rise angle of the churn blade can be designed according to the change of the rotating radius.

Test design

EDEM simulation test

In order to visualize the mixing pattern of material in the flow

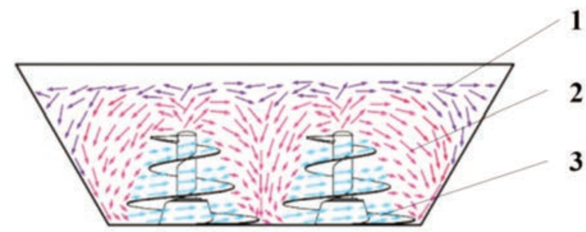

Figure 4. Diagram of the mixing process. 1) Stranded layer; 2) permeable layer; 3) driving layer.

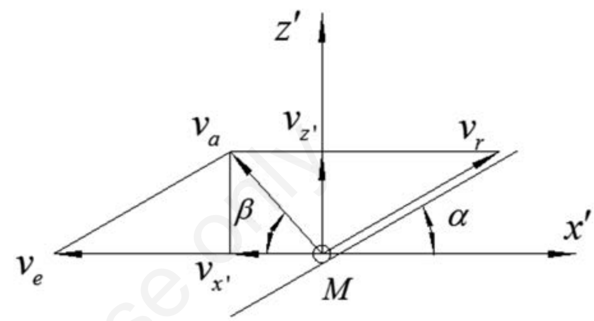

Figure 5. Motion analysis of mixed material. v_e is the convected velocity of churn blade relative to the motion of mixing tank, m·s^{-1}; vr is the relative velocity of M relative to motion of churn blade, m·s^{-1}; v_a is the absolute velocity of M relative to motion of mixing tank, m·s^{-1}; v_x' and v_z' are respectively projection of va in the direction of x' and z', that is circumference velocity and axial velocity of M, m·s^{-1}.

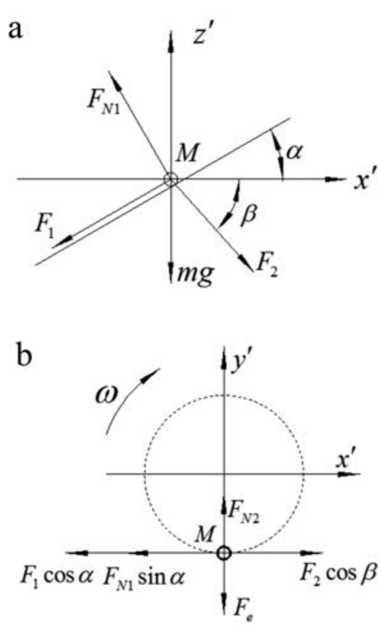

Figure 6. Force analysis of mixed material mg is the gravity of M, N; F_1 is the tangential friction force of stirring blade, N; FN_1 is the support reaction of stirring blade, N; FN2 is the support reaction of outer material, N; F_2 is the shearing force of outer material, N; F_e is the convected inertial force, N. **a**) Force diagram of y' direction; **n**) force diagram of z' direction.

process, the mixing process was simulated by EDEM software. In the simulation experiment, diets were represented by approximately 30% concentrate (corn meal) and 70% roughage (corn silage). The Hertz-Mindlin EDEM default contact mode for the contact model was selected. This model is based on Mindling's research results and has accurate and efficient computational performance. The ideal spherical particle group method is used to approximate the actual material shape instead. The measured data are obtained according to the geometric size of the mixed material and then the average value is obtained. To simplify the simulation model, cornmeal was represented by spherical model particles with a diameter of 0.6 mm. The silage corn was approximated as a cylinder with a diameter of 1 mm and a length of 10 mm using the Hertz-Mindin with bonding particle bonding model. Cornmeal spherical pellets and silage corn models were rendered in red and blue, respectively, for ease of viewing (Teng *et al.*, 2020). Poisson's ratio of material was obtained by consulting the relevant literature. The mechanical properties of material particles, and the geometry and interaction parameters between materials were finally obtained, as shown in *Supplementary Tables 3 and 4*, respectively. In order to simulate closer to the real situation, in accordance with the loading order "first roughage and then concentrate" principle, set the order of generating material particles for silage corn stalks, and cornmeal. Define the mechanical model, specify the calculation area, set the gravitational acceleration, specify the simulation time, and determine the time interval of data saving, mesh size. Then the simulation calculation of the material after completing the above operations was generated. Once the drop simulation was completed, the kinematic properties of the churn device were defined, *i.e.*, the two churns rotated in opposite directions around central axes, after which the simulation of mixing and stirring was carried out.

The purpose of the simulation analysis was to observe the mixing process of the material by the stirring device. The simulation time was set to 30 min in consideration of the huge amount of calculation and the performance of the computer (Guo *et al.*, 2023). Based on the range of mixing parameters derived from the theoretical analysis, a set of mixing processes was simulated for a mixing time of 15 min, a filling coefficient of 70%, and a stirring speed of 50 r/min.

Prototype test

The prototype was tested at an ambient temperature of 25°C and an ambient humidity of 35%. About 70% corn silage (60~70% moisture content) and about 30% concentrate feed (cornmeal, other additives) were used as test material. The tracer method was used to determine the homogeneity of the material. The closer the physical properties of the tracer with the concentrate, the lower the tendency to segregate and the easier to be mixed (Han *et al.*, 2022). Corn kernels were selected as tracers. The kernels were cleaned and processed before addition to ensure that their seeds were uniformly full and free of defects. 4% of the total amount of test material was placed at the same time as the concentrate feed in the front, center, and rear positions of the mixing box. The test site is shown in Figure 8.

Test indicators and measurement methods

Mixing uniformity

After each mixing batch of test material was blended, 70% of the discharge door was opened and 5 samples were taken at 10s intervals at the discharge port. The tracers were then sorted, and the number of tracer grains counted. The mass of each sample was weighed (Li, 2021). The mixing uniformity of the samples was calculated according to Eqs. 10-12.

$$\bar{X} = \frac{\sum_{i=1}^{m} X_i}{m} \tag{10}$$

$$S = \sqrt{\frac{\sum_{i=1}^{n}\left(X_i - \bar{X}\right)^2}{n-1}} \tag{11}$$

$$Y_1 = \left(1 - \frac{S}{\bar{X}}\right) \times 100\% \tag{12}$$

where S is the sample standard deviation; n is the number of samples; m is the number of measurements; X_i is the number of tracer plasmids in the sample as a percentage of the sample mass (%); $\bar{X}$ is the mean value of the percentage of the number of tracer plasmids in the sample compared to the sample mass (%); Y_1 is the mixing uniformity (%).

Roughage particle size

The length of palatable roughage in the whole mixed diet of dairy cows is generally 1~5 cm. The larger the proportion of palatable length roughage in the total roughage, the more favorable it is for the cows to eat (Boerman *et al.*, 2021). Therefore, the ratio of palatable length roughage mass to total roughage mass was selected as the evaluation index of roughage particle size. After each mixing batch of test material had been blended, 70% of the discharge door was opened and 5 samples were taken at 10 s intervals at the discharge opening. Then sieving was carried out using perforated sieves with apertures of 19 mm, 8 mm, and 5 mm, respectively, to separate the palatable length of roughage from the other

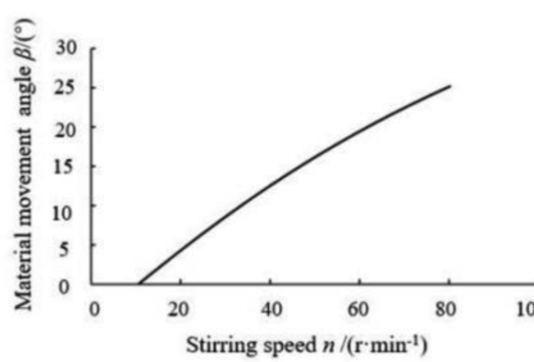

Figure 7. Change curve of material movement angle with stirring speed.

Figure 8. Testing site.

lengths of roughage. The two portions of roughage were weighed separately.

The roughage particle size is calculated as follows:

$$Y_2 = \frac{m_1}{m_1 + m_2} \times 100\% \tag{13}$$

where Y_2 is the roughage particle size (%); m_1 is the mass of roughage with a length of 1 to 5 cm (g); m_2 is the sum of mass of roughage less than 1 cm and more than 5 cm in length (g).

Ton material energy consumption

The prototype was powered by a tractor. In order to measure the energy consumption of ton material energy consumption per mixing batch, a connecting frame was set up between the preparation machine and the tractor. A torque power meter was placed at the connecting frame, which connected the drive shaft of the preparation machine to the power output shaft of the tractor. The power values were measured with the torque power meter are recorded every 1 min.

The ton material energy consumption per mixing batch is calculated as follows:

$$Y_3 = \frac{50\sum W_i}{3Q_c} \tag{14}$$

where Y_3 is the ton material energy consumption (kW·h/t); W_i is the power value measured by the first recorded torque power meter (kW); Q_c is the total mass of test material (kg).

Test program design

By analyzing the mixing mechanism of the double-helix TMR preparation machine, the stirring speed, mixing time, and filling coefficient were taken as the influencing factors. The mixing uniformity, roughage particle size, and ton material energy consumption were taken as the evaluation indexes.

The stirring speed, mixing time, filling coefficient, mixing uniformity, roughage particle size, and ton material energy consumption are expressed as x_1, x_2, x_3, y_1, y_2, and y_3, respectively. X_1, X_2, and X_3 are coded values for the stirring speed, mixing time, and filling coefficient, respectively. According to the pre-test, the range of values of the test factors was determined as follows: stirring speed of 10~50 r/min, mixing time of 10~20 min, and filling coefficient of 30~70%. A three-factor, five-level quadratic regression orthogonal rotating combination test was used (Kronqvist *et al.*, 2021), with factor coding levels (*Supplementary Table 5*). Each set of tests was repeated three times and the average of the results of the three tests was taken. The experimental scheme was designed and the results were analyzed by Design-Expert 10.0.1 software (Damborg *et al.*, 2019; Qi *et al.*, 2017). Schemes and results of experiments are listed in *Supplementary Table 6*.

Results and Discussion

Simulation test analysis

The effect of mixing at different moments is shown in 9. Figure 9a-c represents the distribution of particles at 2 s, 15 s, and 30 s, respectively.

In Figure 9a, there was a clear delamination between the particles at 2 min, with mild penetration between the particle layers. Due to the role of the churn, the driving layer material was gradually lifted upward. The bottom of the mixing tank would be part of the space, resulting in the upper layer of material downward infiltration. Then the permeable layer was present.

In Figure 9b, an obvious diffusion phenomenon between the particle layers can be observed at 15 min. The compartmentalization between layers was broken. The various particle layers were interpenetrated, doped, and mixed with each other.

In Figure 9c, the mixing homogeneity between particles continued to increase at 30 min, with more turbulence between the various particles.

In summary, it can be seen that mixing becomes more and more effective with increasing mixing time. The double-helix TMR machine can realize the full mixing of material, but the best working parameters need to be obtained through tests.

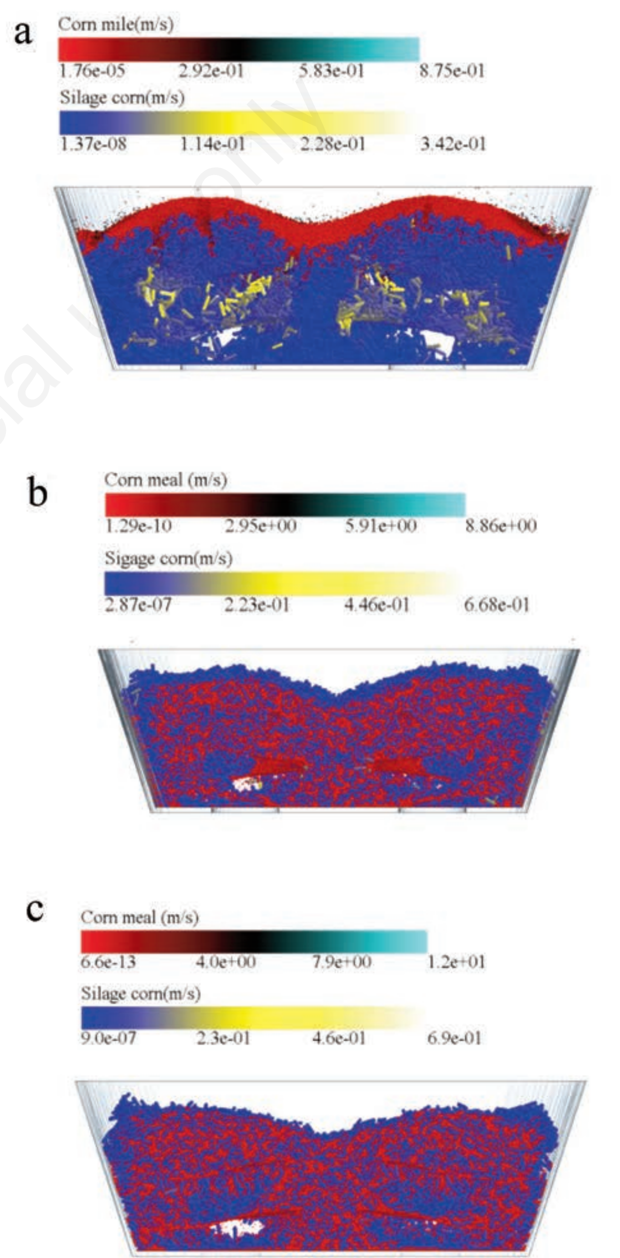

Figure 9. Particle distribution at different moments. **a**) 2 min; **b**) 15 min; **c**) 30 min.

Prototype test analysis

Establishment of regression model and significance analysis of evaluation index

Quadratic regression analysis of the experimental results was carried out using Design-Expert 10.0 software. The multiple regression was fitted to obtain quadratic polynomial response surface regression models with mixing uniformity, roughage particle size and ton material energy consumption as the response functions, respectively. Each factor was taken as the independent variable. The regression Equations are shown in Eqs.15-17.

$$\begin{aligned}Y_1 &= 92.17 + 0.44X_1 + 0.27X_2 + 0.43X_3 - 0.35X_1X_2 - 0.5X_1X_3 \\ &\quad -0.44X_2X_3 - 0.87X_1^2 - 1.38X_2^2 - 0.69X_3^2\end{aligned} \tag{15}$$

$$\begin{aligned}Y_2 &= 71 + 3.35X_1 + 2.29X_2 - 1.41X_3 - 0.48X_2X_3 - X_1X_3 \\ &\quad +0.036X_2X_3 + 0.47X_1^2 + 0.69X_2^2 - 0.087X_3^2\end{aligned} \tag{16}$$

$$\begin{aligned}Y_3 &= 3.67 + 0.25X_1 + 0.74X_2 - 1.12X_3 + 0.03X_1X_2 + 0.12X_1X_3 \\ &\quad -0.21X_2X_3 - 1.742\times10^{-3}X_1^2 + 3.739X_2^2 + 0.16X_3^2\end{aligned} \tag{17}$$

The results of the experiment were analyzed by ANOVA, as shown in *Supplementary Table 7*. The P-value for each indicator model is less than 0.001, indicating that the models are all extremely significant.

The P-value of the lack-of-fit test for each evaluation index was greater than 0.05 (0.7225, 0.9095, 0.1055), indicating that the regression Equations were very well fitted. The determination coefficients R^2-values of the evaluation indexes were 0.9930, 0.9914, and 0.9991 respectively, indicating that the models can explain more than 99.3%, 99.14%, and 99.91% of the evaluation indexes, respectively. Therefore, the operating parameters of the double-helix TMR preparation machine can be optimized using the obtained model. Each regression term for mixing uniformity was significant. Therefore, only the regression terms for the other two evaluation indexes were optimized. The insignificant terms with a small probability (P>0.05) were excluded to obtain the final regression Equation, as shown in Eqs. 18 and 19.

$$\begin{aligned}Y_2 &= 70.95 + 3.35X_1 + 2.29X_2 - 1.14X_3 - 0.48X_2X_3 \\ &\quad X_1X_3 + 0.47X_1^2 + 0.69X_2^2\end{aligned} \tag{18}$$

$$\begin{aligned}Y_3 &= 3.67 + 0.25X_1 + 0.74X_2 - 1.12X_3 + 0.12X_1X_3 \\ &\quad -0.2X_2X_3 + 0.16X_3^2\end{aligned} \tag{19}$$

Main effects analysis

The purpose of the main effects analysis is to determine the importance of the influence of each factor on the mixing performance of the preparation machine. The regression Equation for the test indicators was a multivariate nonlinear model (Zhang *et al.*, 2023). Therefore, the factor contribution ratio was used to determine the relative importance of each factor to the evaluation indexes. The contribution rate and ranking of factors under each evaluation index are shown in *Supplementary Table 8*.

Response surface analysis

The response surface diagram was obtained after data processing to intuitively analyze the relationship between various experimental factors as shown in Figures 10-12.

Mixing uniformity

In Figure 10a, at each level of the mixing time, the mixing uniformity tended to increase and then decrease with the increase of the stirring speed; the mixing uniformity tended to increase and then decrease with the increase of mixing time at all levels of stirring speed.

In Figure 10b, the mixing uniformity increased and then decreased with the increase of stirring speed, and increased and then decreased with the increase of filling coefficient.

In Figure 10c, the mixing uniformity tended to increase and then decrease with the increase of stirring speed, and increased and then decreased with the increase of filling coefficient.

When the mixture of material reaches a homogeneous state, if the material continued to be turned, the material between the components would be separated and graded due to differences in physical properties, resulting in a reduction in mixing uniformity. Increasing the filling coefficient can make the convective mixing more frequent, and accelerate the homogeneous mixing of material. However, when the height of the mixed material in the mixing

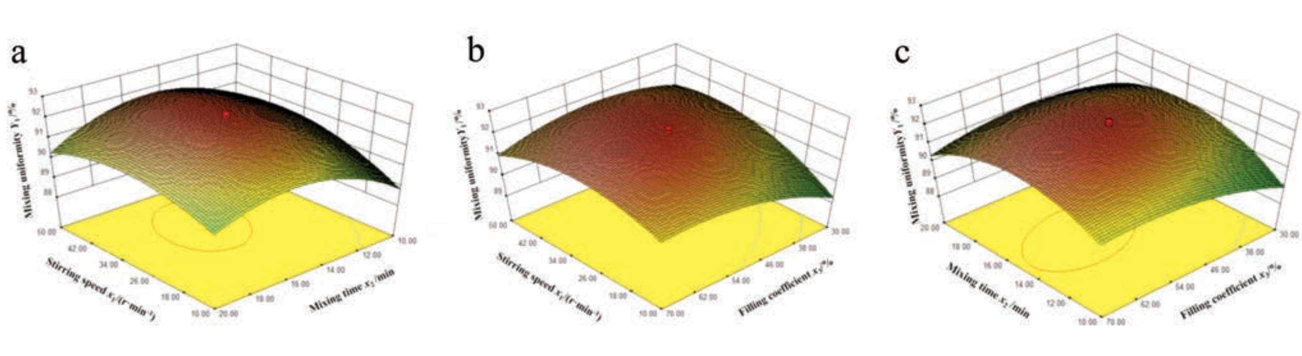

Figure 10. Influence of different factors on mixing uniformity. Note: factors levels of response surface test are shown in *Supplementary Table 4,* and response values are shown in *Supplementary Table 5.*

tank exceeded the top of the churn, the spiral blade could not act directly on this part of the material, then its fluidity was reduced. At the same time, the part of the material would also hinder the churn blade top material throwing, affecting the overall material mixing, resulting in a reduction in the uniformity of mixing.

Roughage particle size

In Figure 11a, the roughage particle size increased with increasing mixing time and with increasing stirring speed. In Figure 11b, the roughage particle size increased with increasing stirring speed and decreased with increasing filling coefficient. The size of the roughage depended mainly on the shearing action of the churn unit on the roughage.

The increase in stirring speed increased the shearing force between the movable blade and the fixed knife. Whereas at lower stirring speeds, the shearing force between the movable blade and the fixed knife cannot reach the cutting force for roughage. The longer the mixing time, the greater the shearing frequency of the blade on the roughage, which was the main reason for affecting the roughage particle size. The increase in the filling coefficient resulted in more material between the spiral blade and the mixing tank, which increased shearing force between the movable blade and the fixed knife, thereby increasing the roughage particle size.

Ton material energy consumption

In Figure 12a, the ton material energy consumption decreased with the increase of the filling coefficient and increased with the increase of stirring speed. In Figure 12b, the ton material energy consumption decreased with the increase of the filling coefficient and increased with the increase of mixing time.

The energy consumption of the tractor was mainly used to drive the churn to rotate and overcome the resistance of the material. It was positively correlated with the mass of the material and the stirring speed of the churn when other circumstances were certain.

Parameter optimization and experimental validation

According to the requirements of the technical specification for quality evaluation of TMR preparation machines (NY/T 2203-2012), mixing uniformity ≥85%, and ton material energy consumption ≤4.2 kW·h/t. The higher the particle size of roughage, the better it is for ruminant animals to feed on it. Generally, more than 70% is required (Wei *et al.*, 2021). The optimal constraint was as follows:

$$\begin{cases} \max Y_1 \\ \max Y_2 \\ \min Y_3 \\ s.t\begin{cases} 10r/\min \le x_1 \le 50r/\min \\ 10\min \le x_2 \le 20\min \\ x_3 = 70\% \end{cases} \end{cases} \tag{20}$$

Through the solution of the Design-Expert 10.0 1 software, the best combination was found. When the stirring speed, mixing time,

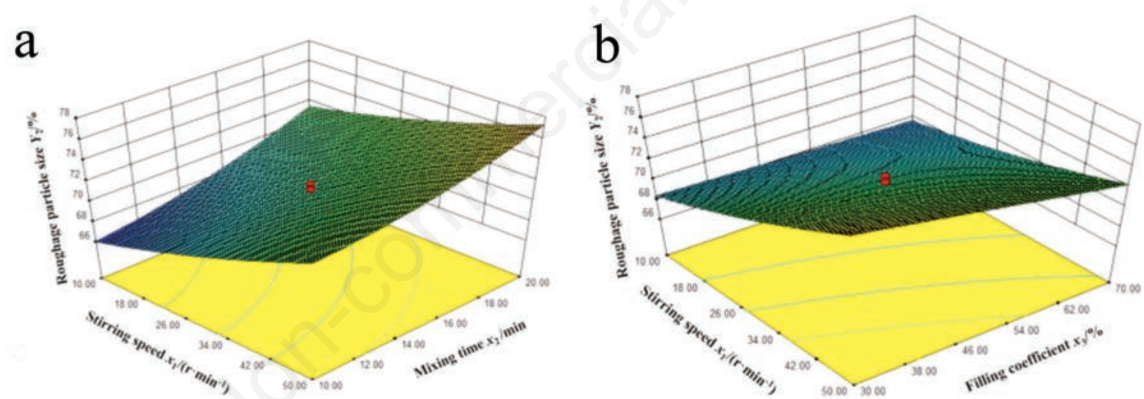

Figure 11. Influence of different factors on roughage particle size. a) Y2 (X1, X2, 0); a) Y2 (X1, 0, X3).

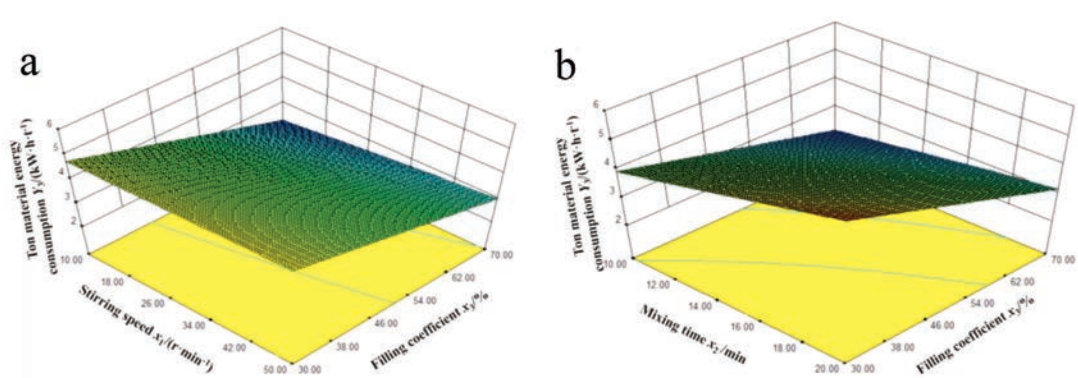

Figure 12. Influence of different factors on ton material energy consumption. a) Y3(X1, 0, X3); b) Y3(0, X2, X3).

and filling coefficient were 48.59 r/min, 14.98 min, and 70%, the corresponding mixing uniformity, roughage particle size, and ton material energy consumption were 91.62%, 70.03%, and 2.93 kW·h/t. This experimental result is significantly better than the self-propelled TMR preparations mixer for silage straw feed designed by Tian *et al*. (2020b), and Wang (2022). Compared with the vertical single-helix structure, the double-helix has more advantages in mixing uniformity (Dong *et al*., 2019). It depends on the blade of the double helix to shear the material around. Compared to the paddle-type ration mixer (Wang *et al*., 2020), the structure has a larger volume and is more suitable for practical production. The horizontal TMR preparation machine (Guo, 2023) is low in height and easy to take material. However, the material mixing effect is poor, and the material is easy to accumulate at the bottom of the tank.

In order to verify the accuracy of the optimized parametric model, simulations were carried out using the optimized parameters. Considering the practical structural design and the feasibility of the test, the stirring speed was set at 48.6 r/min, the mixing time was 15 min, the filling coefficient was 70% (*Supplementary Table 9*). The results showed that the error of each evaluation index was less than 3%, the predicted and experimental values were in good agreement. It can be seen that the model has high prediction accuracy, which indicates that the optimization results can be used as the optimal working parameters of the double-helix TMR preparation machine.

Conclusions

Aiming at the single form, low efficiency, uneven mixing, and other problems of the domestic TMR preparation machine, a double-helix TMR preparation machine was designed. The churning device consists of a pair of vertical conical churns with opposite rotations, which can realize full mixing of the ration. By analyzing the mixing mechanism of the preparation machine, the influencing factors and ranges affecting the mixing performance of the preparation machine were obtained. The EDEM discrete element simulation test verified the mixing effect of the preparation machine material.

The three-factor and five-level central composite design center combination orthogonal rotary test in the prototype was carried out with stirring speed of the churn, mixing time, and filling coefficient as influencing factors, mixing uniformity, roughage particle size, and ton material energy consumption as evaluation indexes. The test results showed that the contribution of each factor to the mixing uniformity in descending order was filling coefficient, stirring speed, and mixing time, to the roughage particle size was stirring speed, mixing time, and filling coefficient, and to the ton material energy consumption was filling coefficient, mixing time and stirring speed. In addition, the mixing uniformity, roughage particle size and ton material energy consumption were obtained as 91.11%, 72.13%, and 2.99 kW·h/t using a response surface analysis. The relative error for all evaluation indexes between the experimental results with round parameter combination and the predicted value was verified to be less than 3%. All the indexes were better than the relevant national standards. Therefore, the research results of this paper can provide data reference and technical support for the design and selection of operating parameters of TMR preparation machines.

Although this paper has done a certain degree of research on the double-helix TMR preparation mixer for silage straw feed, there are still some shortcomings, and further research and upgrading of the preparation mixer are needed.

The cutting and kneading effect of the movable blade installed on the spiral blade will affect the quality of the whole mixed diet, which can be studied and improved in the future;

For the simulation analysis of material mixing performance, each simulation takes too long because there are too many particles in the actual working condition. In the follow-up study, the particle model should be further optimized to make the simulation results more realistic;

The selection of some mechanical property parameters is set by referring to the existing literature data, so there may be some deviation between the simulation results and the actual situation. In the subsequent research, various material simulation parameters can be accurately selected through test determination.

References

Chen, M.Y., Wang, B.X., Fan, G.Q., Dong, H.Y., Wang, Z.Y., Wang, Y.L. 2022. Design and experiment of loading elevator of self-propelled TMR preparation mixer. Transact. Chin. Soc. Agric. Mach. 53:148-57.

Damborg, V.K., Jensen, S.K., Johansen, M. 2019. Ensiled pulp from biorefining increased milk production in dairy cows compared with grass–clover silage. J. Dairy Sci. 102:8883-97.

Dong, H.Y., Teng, X., Fan, G.Q., Jiang, J.P., Qi, Z.C., Han, J. 2019. Design of 9JGL-12 total mixer rotation mixer. Xinjiang Agric. Mechan. (6):32-7.

Frizzarin, M., O'Callaghan, T.F., Murphy, T.B., Hennessy, D., Casa, A. 2021. Application of machine-learning methods to milk mid-infrared spectra for discrimination of cow milk from pasture or total mixed ration diets. J. Dairy Sci. 104:12394-402.

Guo, X. 2023. Mixing simulation and key parameters optimization of horization total mixed ration mixer. Ningxia University, Yin Chuan.

Guo, Z.F., Ma, Y., Shen, W.Q., Ban, T. 2023. Design and finite element analysis for the material mixer of cotton straw feed fermentation equipment. Feed Industry Magazine. 44:07-11.

Han, B.B., Ren, Z.Y., Zhang, D.F., Kuai, L.J. 2022. Force analysis and optimization of TMR mixer auger. Ningxia Eng. Technol. 21:75-9.

Jiang, Y.J., Cao, Z.H., Wen, Y.C., Zhang, C. Shi, X. 2022. Simulation analysis on rotary process of herringbone blade feed mixer. J. Wuhan Polytech. Univ. 41:90-5+119.

Kronqvist, C., Petters, F., Robertsson, U., Lindberg, M. 2021. Evaluation of production parameters, feed sorting behaviour and social interactions in dairy cows: comparison of two total mixed rations with different particle size and water content. Livestock Sci. 251:104662.

Li, W., Wen, B., Song, P. 2021. Power consumption analysis and experimental study on the kneading and cutting process of licorice stem in horizontal total mixed ration mixer. Processes. 9:2108.

Li, L.Q., Wang, D.F., Li, C. 2017. Mixing process analysis and performance experiment of rotary ration mixer. Transact. Chin. Soc. Agric. Machin. 48:123-32.

Li, W., Wen, B., Song, P. 2021. Power consumption analysis and experimental study on the kneading and cutting process of licorice stem in horizontal total mixed ration mixer. Processes. 9:2108.

Niu, Q.Q., Wang, B.X., Dong, H.Y., Fan, G.Q., Wu, A.B. Liu, M.

2022. Feeding simulation and parameter optimization of self-propelled total mixed ration preparation machine. J. Chin. Agric. Mechan. 43:99-106.
Qi, J.T., Meng, H.W., Kan, Z., Li, C.S., Li, Y.S. 2017. Analysis and test of feeding performance of dual-spiral cow feeding device based on EDEM. Transact. Chin. Soc. Agric. Eng. 33:65-71.
Schingoethe, D.J. 2017. A 100-year review: total mixed ration feeding of dairy cows. J. Dairy Sci. 100:10143-50.
Sun, B.Z., Bai, Y., Wu, Y.L., et al. Technical specification of quality evaluation for total mixer. Agricultural industry standard of the People's Republic of China, NY/T 2203-2012.
Teng, X., Dong, H.Y., Fan, G.Q., Wu, A.B., Han, J., Jiang, J.P. 2020. Design and test of spiral wringing dragon type cattle research muck cleaner. J. Chin. Agric. Mechan. 41:42-7.
Tian, F.Y., Chen, Y.H., Song, Z.H., Yan, Y.F., Li, F.D., Wang, Z.H., Xiong, B.H. 2020a. Finite element simulation and performance test of loading and mixing characteristics of self-propelled total mixed ration mixer. J. Eng. pp. 1-15.
Tian, F.Y., Chen, Y.H., Song, Z.H., Yan, Y.F., Li, F.D. Wang, Z.H. 2020b. Design and experiment of self-propelled TMR preparation mixer for silage straw feed. Transact. Chin. Soc. Agric. Machin. 51:106-114.
Wang, B.X. 2022. Design and optimization of self-propelled total mixed ration preparation machine. Shandong Agricultural University, Taian.
Wang, D.F., Li, C., Li, L.Q. 2017a. Mechanism analysis and parameter optimization of hammer mill for corn stalk. Transact. Chin. Soc. Agric. Machin. 48:165-71.
Wang, D.F., Wang, M., Li, L.Q. 2017b. Mechanism analysis and parameters optimization of hammer mill for corn stalk. Transact. Chin. Soc. Agric. Machin. 48:165-71.
Wang, D.F., Dang, C.X., Huang, H.N., Liu, C.X. 2020. Mechanism analysis and parameter optimization of paddle-type ration mixer. Transact. Chin. Soc. Agric. Machin. 51:122-31.
Wang, K.F., Wen, B.Q., Yellubye, A., Zhang, J., Li, L.Q., Li, Y., Li, J.B., Kan, K. 2020. Research on the influence of the screw structure of the segmented spiral TMR mixer on the mixing performance based on the discrete element method. Feed Industry Magazine. 41:35-41.
Wang, Z.T., Yu, W.J., Liu, Y., Tang, Y.R., Niu, H., Lan, H.P., Zhang, Y.C. 2019. Optimization of process parameters for particle mixing in spiral mixer. Feed Industry Magazine 40:6-10.
Wei, Y.Z., Zhang, J, Xue, M. 2021. Structural design and roughage size test of total mixed ration machine. Agric. Equip. Vehicle Eng. 59:66-9.
Zhang, H.Y., Li, Y., Wu, L.L., Liu, J.X., Bi, J.H. 2023. Preparation of a kind of mixed silage and its research progress in cow production. China Feed (2):5-8.

Online supplementary material:
Table S1. Advantages and disadvantages of total mixed ration mixer.
Table S2. Main technical parameters of the double-helix total mixed ration preparation mixer.
Table S3. Material mechanical properties.
Table S4. Properties of material interactions.
Table S5. Coding and level of experimental factors.
Table S6. Schemes and results of experiment.
Table S7. Significance test of the model.
Table S8. Importance of effects of factors on response functions.
Table S9. Comparison between model optimization and validation test value.